

<https://helda.helsinki.fi>

---

## Impact of doping and silicon substrate resistivity on the blistering of atomic-layer-deposited aluminium oxide

Ott, Jennifer

2020-08-30

---

Ott, J, Pasanen, T P, Gadda, A, Garin, M, Rosta, K, Vahanissi, V & Savin, H 2020, 'Impact of doping and silicon substrate resistivity on the blistering of atomic-layer-deposited aluminium oxide', Applied Surface Science, vol. 522, 146400. <https://doi.org/10.1016/j.apsusc.2020.146400>

---

<http://hdl.handle.net/10138/347550>

<https://doi.org/10.1016/j.apsusc.2020.146400>

---

cc\_by\_nc\_nd

acceptedVersion

---

*Downloaded from Helda, University of Helsinki institutional repository.*

*This is an electronic reprint of the original article.*

*This reprint may differ from the original in pagination and typographic detail.*

*Please cite the original version.*

# Impact of doping and silicon substrate resistivity on the blistering of atomic-layer-deposited aluminium oxide

*Jennifer Ott<sup>1,2,\*</sup>, Toni P. Pasanen<sup>2</sup>, Akiko Gädda<sup>1</sup>, Moisés Garín<sup>2,3</sup>, Kawa Rosta<sup>2</sup>, Ville Vähänissi<sup>2</sup>, Hele Savin<sup>2</sup>*

<sup>1</sup> Helsinki Institute of Physics, Gustaf Hällströmin katu 2, FI-00014 University of Helsinki, Finland

<sup>2</sup> Aalto University, Department of Electronics and Nanoengineering, Tietotie 3, FI-02150 Espoo, Finland

<sup>3</sup> GR-MECAMAT, Universitat de Vic – Universitat Central de Catalunya, Campus Torre dels Frares, c/ de la Laura 13, ES-08500 Vic, Spain

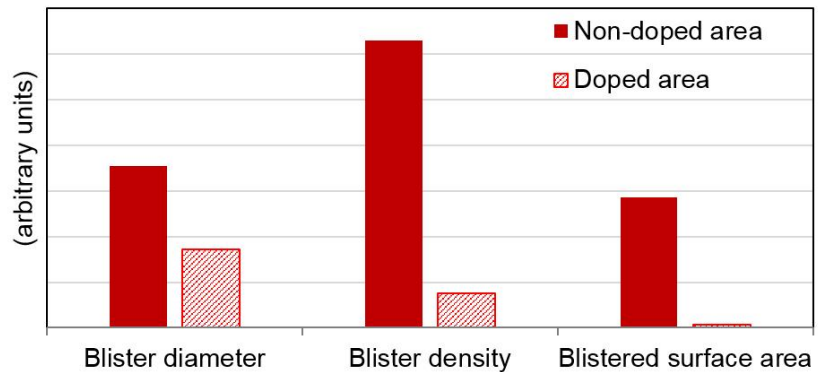
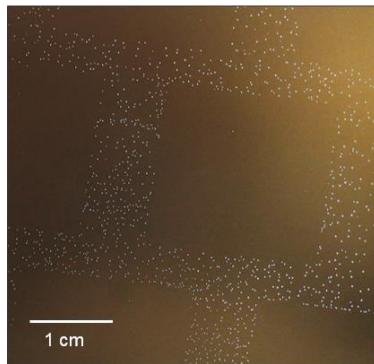
\* corresponding author. E-mail: [jennifer.ott@aalto.fi](mailto:jennifer.ott@aalto.fi)

Keywords: aluminium oxide, silicon, surface passivation, doping, blistering

---

Aluminium oxide (Al<sub>2</sub>O<sub>3</sub>) thin films grown at low temperatures using atomic layer deposition (ALD) are known to often suffer from local delamination sites, referred to as “blisters”, after post-deposition annealing during device processing. In this work, we report our observation that doping of the silicon substrate has an effect on blister formation. The introduction of a highly doped layer by diffusion or implantation is found to significantly reduce blistering, compared to the non-doped regions in the immediate vicinity. Similar behavior is observed for both phosphorus and boron doping. Further investigation of this phenomenon using substrates with different resistivities reveals that even when introduced already during silicon crystal growth, doping affects the blistering of aluminium oxide films. Changes in several properties of silicon affected by doping, most importantly surface terminating groups, native oxide growth, and passivation of defects with hydrogen, are discussed as potential reasons behind the observed effect on blistering.

**TOC / Graphical abstract:**



**(left)** Photograph of a high-resistivity n-type Si wafer coated with 50 nm of ALD-grown aluminium oxide, with clearly reduced blistering in the 2×2 cm<sup>2</sup> areas implanted with boron.

**(right)** Comparison of blister properties in areas with diffused emitter and surrounding areas.

**Highlights**

- The impact of doping in silicon on blistering of Al<sub>2</sub>O<sub>3</sub> thin films is investigated
- Diffusion and implantation of the silicon substrate significantly reduce blistering
- Blistering is affected even by doping during crystal growth
- Increasing substrate resistivity promotes fewer, but larger blisters

## 1. Introduction

During the past decades, atomic layer deposition (ALD) has grown into a key technology for microelectronics and photonics, enabling the growth of thin films at nanoscale precision with excellent conformality and uniformity [1]. Dielectrics with a significant effective charge, such as aluminium oxide ( $\text{Al}_2\text{O}_3$ ), are frequently employed as surface passivation layers in optoelectronic devices, most prominently in solar cells [2].  $\text{Al}_2\text{O}_3$  has also found application in radiation detectors, where it can serve as capacitor dielectric in highly segmented strip and pixel sensors [3,4,5].

An unwanted property reported for ALD thin films, especially for  $\text{Al}_2\text{O}_3$  films deposited from trimethylaluminium (TMA) and water precursors, is the formation of local delamination sites, referred to as “blisters”. Increased blistering has been found to correlate with degraded surface passivation and decreased open-circuit voltage ( $V_{oc}$ ) in silicon solar cells [6,7,8,9]. In a complex segmented device, such as a pixel detector, ruptured blisters present a severe risk of short-circuits between elements in the detector, which may render the device non-functional [10]. While most studies consider blisters as detrimental for device operation, the usage of blisters as contact openings in Al BSF solar cells has been described as well [11].

Blisters usually arise during post-deposition annealing of the thin films: although ALD processes are performed at relatively low temperatures, the films are often exposed to higher temperatures during following device processing steps, such as the sintering and/or firing of metal contacts, or the activation anneal in case of  $\text{Al}_2\text{O}_3$  passivation [12]. Consequently, blistering is widely attributed to the accumulation of hydrogen at the film-substrate interface with  $\text{Al}_2\text{O}_3$  acting as an outgassing barrier [12-14], but has also been linked to chemical reactions at the Si surface [15] and local cavitation of the silicon substrate [15, 16]. However, the exact mechanism, or mechanisms, of blister formation is not known with certainty, and a wide variety of factors have been reported to

affect the formation of blisters. ALD parameters, such as deposition temperature [17], oxygen precursor [18], and film thickness [18], have been found to influence blistering of  $\text{Al}_2\text{O}_3$ , as well as time and temperature range [7,19] and also the ambient [8] of post-deposition anneal treatments. In addition, blistering is affected by modification of the silicon substrate surface by oxidation [20], chemical cleaning [21], or plasma treatment [6].

As a further addition to the factors described above, during device fabrication, we observed that localized doping of the silicon substrate, in this case ion implantation with phosphorus on the patterned front side, caused a visible change in the blistering behavior of  $\text{Al}_2\text{O}_3$  films. An impact of doping on the blistering of thin films has not been reported before, and requires a more detailed investigation in order to improve our understanding of the blistering behavior of  $\text{Al}_2\text{O}_3$  films.

In this work, we study the impact of doping in silicon on  $\text{Al}_2\text{O}_3$  blistering in terms of blister size, density and total surface area covered by blisters, using unpatterned  $\text{Al}_2\text{O}_3$  thin films grown by ALD. The effect of localized external doping by diffusion and ion implantation with boron and phosphorous is investigated. To study the role of doping concentration only, without impact from any external doping method, further experiments are conducted using a series of silicon substrates with various bulk resistivities. Our primary focus lies on phosphorus-doped samples due to the prevalence of p-type substrates in silicon photovoltaics as well as in future detectors for high-energy physics, which employ a phosphorus-doped layer on the front side to form the p-n junction, but also boron-doped samples are studied in order to look for differences in blistering behavior with dopant type.

## 2. Experimental

### 2.1. Sample preparation

Three sets of samples were prepared to study the effects of diffusion, ion implantation, or bulk resistivity on  $\text{Al}_2\text{O}_3$  blistering. Figure 1 presents a schematic view of the sample fabrication flow.

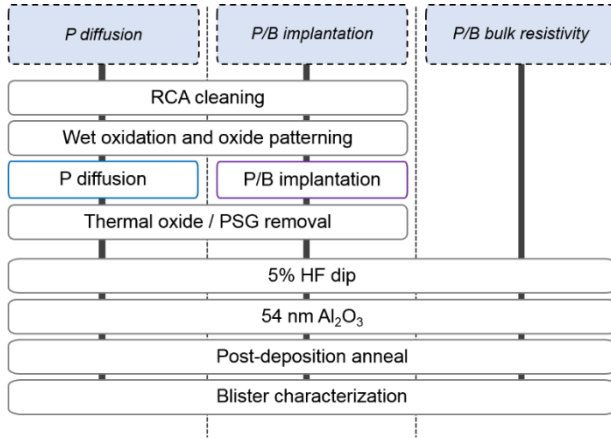


**Figure 1.** Schematic view of the fabrication flow for samples with different external doping or bulk resistivity.

Samples for diffusion and implantation experiments were first subjected to standard RCA cleaning [22] and then wet oxidized at 1000 °C to obtain thermal oxides of 400-500 nm thickness as hard mask layer. The oxide layer was patterned by buffered hydrofluoric acid (BHF) wet etching, with a design of seven  $2 \times 2 \text{ cm}^2$  square openings distributed over a 4" wafer surface area.

Phosphorus diffusion was performed at 830 °C as described in [23], by a 20 min exposure of phosphorus oxychloride ( $\text{POCl}_3$ ) with subsequent 5 min drive-in in  $\text{O}_2$  ambient.

Implantation was performed in an Eaton-NV-3206h Ion Implanter with surface doses of  $1 \times 10^{15} \text{ cm}^{-2}$  for both phosphorus (60 keV) and boron (30 keV) ions. Afterwards, the mask oxide was removed, the wafers were again RCA-cleaned, and the ions were driven into the bulk at 1100 °C for 46 min in dry oxidation conditions.

Samples with different bulk resistivity did not receive any pre-treatment except a 2-3 min dip in 5 % HF to remove the native SiO<sub>2</sub> layer prior to ALD and to create a H-terminated surface.

The thermal oxide or phosphosilicate glass layers of the implantation and diffusion samples, respectively, were also removed by 3 min etching in 5 % HF, in order to ensure similar surface conditions as in the base doping samples.

An overview of the bulk resistivities and doping concentrations of the samples studied here is presented in Table 1.

**Table 1.** Overview of samples. Surface concentrations in the top part of the table are calculated as electrically active dopants from bulk resistivities. For implanted/diffused samples in the bottom rows, surface concentrations are total dopant concentrations based on implantation dose and profiles.

| Bulk dopant | Crystal growth method | Substrate crystal orientation | Bulk resistivity ( $\Omega\text{cm}$ ) | External surface dopant (doping method) | Concentration at the surface ( $\text{cm}^{-3}$ ) |
|-------------|-----------------------|-------------------------------|--|---|---|
| <b>P</b>    | HPS-Fz                | (111)                         | 3000-7000                              | -                                       | 6.3e11 - 1.5e12                                   |
| <b>P</b>    | Cz                    | (100)                         | >500                                   | -                                       | < 8.8e12  |
| <b>P</b>    | Cz                    | (100)                         | 1-20                                   | -                                       | 2.2e14 - 4.9e15                                   |
| <b>P</b>    | Cz                    | (111)                         | 0.005-0.1                              | -                                       | 5.0e18 - 1.2e19                                   |
| <b>B</b>    | Cz                    | (100)                         | >10 000                                | -                                       | < 1.3e12  |
| <b>B</b>    | Cz                    | (100)                         | 1-20                                   | -                                       | 6.7e14 - 1.5e16                                   |
| B           | Cz                    | (100)                         | 1-20                                   | <b>P (diff.)</b>                        | 1e20-1e21   |
| B           | Cz                    | (100)                         | >10 000                                | <b>P (impl.)</b>                        | 1e19  |
| P           | HPS-Fz                | (111)                         | 3000-7000                              | <b>B (impl.)</b>                        | 4e18  |

For all samples, Al<sub>2</sub>O<sub>3</sub> deposition was performed in a Beneq TFS-500 batch-type ALD reactor at 200 °C. One ALD cycle consisted of a 400 ms trimethylaluminium (TMA) pulse, followed by a 7

s N<sub>2</sub> purge, then a 500 ms double pulse of DI water, and another final 7 s N<sub>2</sub> purge. This sequence was repeated 500 times, resulting in a film thickness of 54 nm and refractive index 1.64, as determined by ellipsometry. Post-deposition annealing of the films was done in a PEO-601 quartz tube furnace in nitrogen atmosphere at 370 °C for 30 min.

## **2.2. Blister identification and quantification**

Our study made use of a WITec Alpha300 optical microscope with a controllable stage for scanning the sample surfaces, and a circular pattern recognition algorithm to detect blisters and determine their size. A number of randomly selected regions on the sample surface, of size 5x5 mm<sup>2</sup> or 1x1 mm<sup>2</sup> depending on the observed blister size, were scanned with a 20x magnification objective and stitched into a single image, using a functionality of the WITec Suite 5.1 microscope operation software. The black/white scale of these stitched images was adjusted so that blisters were visible with high contrast, and background noise was eliminated. This, in addition to precise focus adjustment, also prevented dust particles or other elevated surface features from affecting blister characterization.

Following image acquisition, an algorithm was used to first identify blisters, which were defined as continuous regions with a certain minimum number of pixels deviating from the background. A circular fit was then applied to each individual pixel cluster, assuming that the blister edges formed a perfect circle and blisters did not overlap. The blister diameter was extracted from this fit.

The validity of this approach was verified by inspection of the fitted images produced by the algorithm. Non-circular, asymmetric delamination areas were found to be very rare. The lower limit of detection with this method, including constraints from image resolution, was approximately



1  $\mu\text{m}$  for blister diameter. Results are reported as blister density, i.e. the number of blisters per unit area, and average diameters with absolute standard deviation as experimental error.

The uncertainty induced by the quality of the fit was judged to be insignificant compared to the intrinsic deviation in blister size over the scanned sample area. The blistered surface area (the ratio of the summed blister area and the total scanned area) was calculated based on the blister count and diameters.

SEM images of blisters were recorded with a Zeiss Supra 40 instrument. Atomic force microscopy was performed with a Veeco Dimension 5000 instrument, using a Nanosensors PPP-NCH n<sup>+</sup> Si scanning probe with a specified spring constant between 10-130 N/m and tip radius of < 10 nm, at a resonant frequency of 290 kHz in tapping mode.

### **3. Results and discussion**

#### **3.1. Influence of external doping**

First, we studied the impact of diffusion or ion implantation on Al<sub>2</sub>O<sub>3</sub> blistering. Observations even by the naked eye strongly indicate that blistering is significantly reduced in doped regions compared to the non-diffused or non-implanted surroundings, with an example given in Figure 2a. This effect was seen in all studied doping methods and species. A closer inspection by scanning electron microscope in Figure 2b confirms that both the blister diameter and blister density are reduced in the region with external doping. More images at higher magnification are provided in the Supporting Information, Section 1.

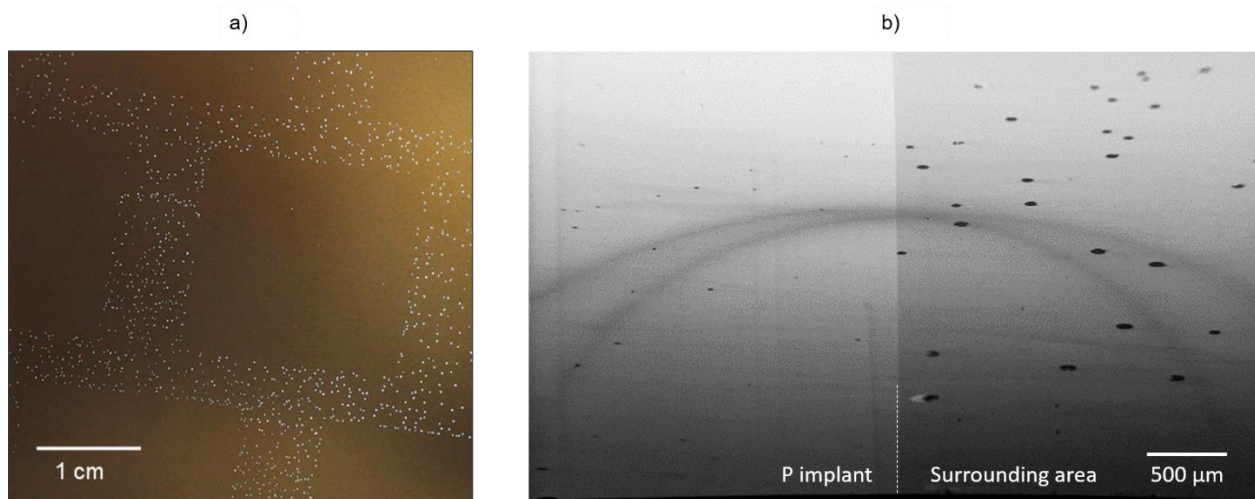


**Figure 2.** a) Photograph of a high-resistivity n-type Si wafer coated with 50 nm of ALD-grown aluminium oxide, with clearly reduced blistering in the  $2 \times 2 \text{ cm}^2$  B-implanted areas. b) SEM image of a high-resistivity p-type Si wafer, with reduced blistering in the P-implanted area (the dark curved line is an optical artifact).

Atomic force microscope scans of the sample surface also show a significant difference in diameter and height of blisters in doped regions, while in both cases blisters retain a regular, circular outline. Figure 3 displays typical blisters on a low-resistivity p-type wafer without and with phosphorus doping implemented by diffusion: in the non-doped region, a blister approximately  $9 \text{ μm}$  in diameter extends up to a height of more than  $0.7 \text{ μm}$ , whereas a smaller blister in the film deposited on an area with diffused phosphorus, remains smaller at around  $3 \text{ μm}$  diameter and  $0.27 \text{ μm}$  in height.

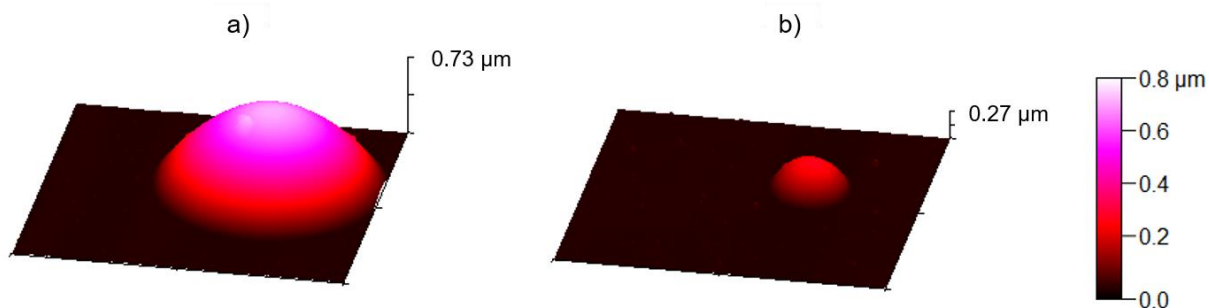


**Figure 3.** AFM scans over  $15 \times 15 \text{ μm}^2$  of a p-type low-resistivity wafer, a) without and b) with a diffused phosphorus layer.

It is notable that in SEM, most blisters appear to be ruptured (i.e. the  $\text{Al}_2\text{O}_3$  film is removed at the blister, cf. Supporting Information), as opposed to optical microscopy and AFM, where the  $\text{Al}_2\text{O}_3$  film is retained in the shape of a partial sphere. This indicates that a blistered  $\text{Al}_2\text{O}_3$  film may be very sensitive to handling and exposure to high vacuum, and can suffer full localized delamination of the film, especially when the blister size is large.

A more detailed analysis of blister properties in the doped regions and their surroundings is based on data obtained with an optical microscope over larger areas providing more statistics, with the results shown in Figure 4.

In the doped regions, blister densities (Fig. 4a) are reduced, most notably from 12.5 to 1.5 blisters/ $\text{mm}^2$  for the sample with diffused phosphorus, and from  $1/\text{mm}^2$  to the point of zero detectable blisters in boron-implanted regions. As an exception, the sample with phosphorus implantation shows a slight increase in blister density to 3 blisters/ $\text{mm}^2$ ; however, a very low density of blisters of  $< 1/\text{mm}^2$  was measured for this sample on the non-implanted surfaces, which limits a reliable comparison to the implanted areas.

Blister diameters (Fig. 4b) are smaller in the doped regions of all examined samples. This effect is especially prominent in both implanted samples, where the average blister diameter is reduced from 50 - 85  $\mu\text{m}$ , respectively, to  $\leq 20 \mu\text{m}$ . In the sample with diffused phosphorus, which exhibits smaller blisters but in turn higher initial blister density than the other samples, the decrease in blister size from around 7  $\mu\text{m}$  is observable, but less pronounced. The total surface area taken up by the blisters (Fig. 4c), finally, is less in the doped areas than in the surrounding regions in all samples, due to the combined contribution of reduced blister densities and blister sizes in the doped areas. The largest blistered surface area remains in the phosphorus-implanted sample, but also there the blistered surface area is reduced approximately by a factor of 2 compared to the non-implanted region.

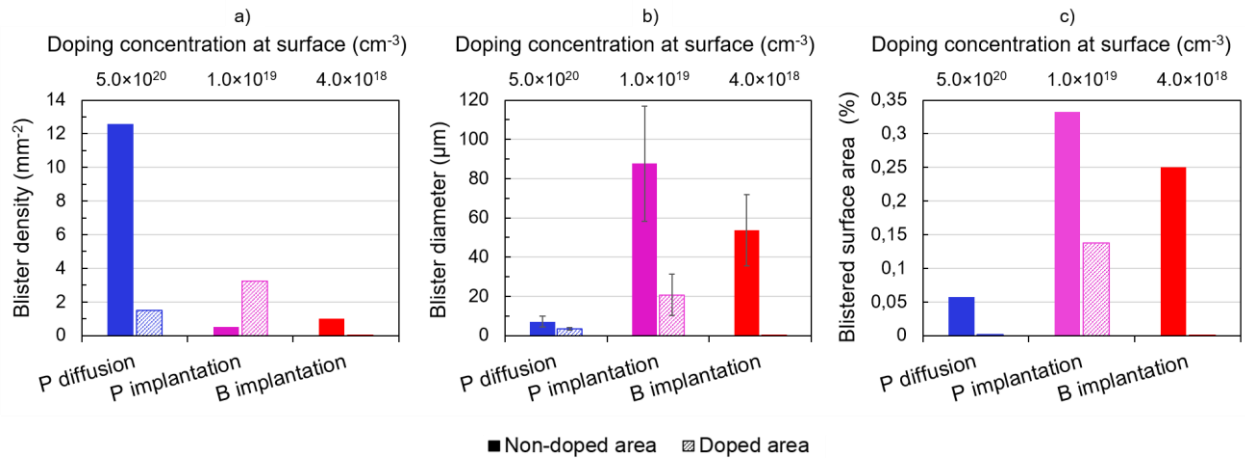


**Figure 4.** Comparison of blistering properties: a) blister density, b) blister diameter, c) blistered surface area, in samples with implanted or diffused emitter regions. The doped area in the B implantation sample did not contain any detectable blisters. Doping concentrations are total dopant concentrations.

A variety of factors connected to the presence of dopant atoms in silicon can be responsible for the observed change in blistering properties, and are discussed in the following text.

The changes in blister characteristics observed here may be connected to the diffusion of gaseous hydrogen or water at the  $\text{Al}_2\text{O}_3$ -Si interface, which has been presented in the literature as the dominant cause for blistering [12,13,14]. It is possible that hydrogen that would otherwise diffuse to the Si-film interface and form blisters if locally exceeding a critical pressure, is instead diffusing to defect states in the Si lattice introduced by external doping. The passivation of both acceptor- and donor-type defects in bulk silicon with hydrogen has indeed been known for a long time [24-27]. Furthermore, the surface mobility of Si atoms, which has been presented as a potential mechanism in  $\text{Al}_2\text{O}_3$  blister formation [16], may be reduced if the substrate contains high concentrations of dopant elements, especially at the surface, as would be the case for implanted and diffused regions.

The absence of detectable blisters in the B-implanted areas provides fewer details for comparison, but indicates that implantation with boron instead of phosphorus has a more significant effect in reducing Al<sub>2</sub>O<sub>3</sub> blistering. Nonetheless, it appears that the blistering behavior of Al<sub>2</sub>O<sub>3</sub> is generally similar in B- and P-implantation samples. This implies that the process of introducing different elements into the silicon bulk, and the method used for this purpose, have a more significant effect on Al<sub>2</sub>O<sub>3</sub> blistering than the differing electrical properties induced by a certain dopant species.

A key difference between diffusion and implantation as doping methods is the resulting total dopant concentration, which is commonly higher in diffused samples [28]. In order to compare the influence of total dopant concentration, Figure 4 includes the total dopant concentrations in the surface region of the silicon substrates on a secondary axis. The results suggest that a higher total dopant concentration at the surface may be connected to both lower blister density and smaller blisters, therefore resulting in a lower surface coverage of blisters.

In addition, the significantly higher concentrations of phosphorus in the diffusion process can promote the formation of characteristic defects, namely electrically inactive phosphorous clusters [23], which are not expected to form in the lower doping concentrations achieved by ion implantation. In contrast, the dominant types of defects introduced by ion implantation, such as vacancies and Frenkel pairs produced by knock-on displacement of the Si atoms upon impact of the high-energy phosphorus atoms, represent point-like damage [28]. Assuming a connection of reduced blistering to enhanced hydrogen diffusion into the bulk, point defects are likely to possess smaller trapping cross-sections and lifetimes than defect clusters. However, if the aforementioned defects are not fully recovered by the high-temperature activation anneal after implantation, they might still play a role in the reduction of blistering on implanted surfaces. The mechanisms of defect formation in boron and phosphorus implantation are very similar, although boron is a lighter atom than phosphorus and is implanted at lower energies, therefore inducing less damage. The

complete absence of blisters in the examined B-implanted area is therefore not explained by defect models related to ion implantation. This is to some extent supported by the probing of bare diffused or implanted silicon surfaces with AFM, when the Al<sub>2</sub>O<sub>3</sub> film was removed after studying the blistering properties, where measurements did not reveal significant changes in roughness compared to the non-diffused or non-implanted surfaces. For all samples, mean roughnesses of doped and non-doped areas were within  $\pm 20\%$  from each other.

Another potential explanation for the effect of doping concentration on blister properties of Al<sub>2</sub>O<sub>3</sub> thin films is a change in surface hydrophilicity, i.e. –H or –OH termination after the pre-ALD HF dip, with substrate doping concentration [29]. Even though the thermal SiO<sub>2</sub>, PSG and native oxide layers were certainly removed by the comparatively long HF etch, which was observed as clear hydrophobicity of the surfaces, the formation of a native SiO<sub>2</sub> layer during the DIW rinse or in air [9,30] may have been enhanced by high substrate doping. This theory is supported by reports that on n<sup>+</sup> Si substrates, the native oxide layer has been reported to be thicker and grow at a faster rate than on n-type substrates [30], an observation also often made in practice during cleaning of highly doped wafers. Thin interfacial SiO<sub>2</sub> layers, chemical or thermal, have in turn been shown to prevent Al<sub>2</sub>O<sub>3</sub> blistering [20,21].

Based on the results presented here, it can also not be ruled out that higher dopant concentrations in the silicon substrate, either chemically or in an electrically active state, directly affect the blistering of Al<sub>2</sub>O<sub>3</sub> films. This question is addressed in the following section.

### **3.2. Effect of silicon substrate bulk resistivity**

A series of substrates with varying bulk resistivities, i.e. with different electrically active doping concentrations established already during crystal growth, was prepared to investigate the dependency of blister size and density on dopant concentration only. Figure 5 shows blister density

and blister diameter with varying substrate bulk resistivity for n-type as well as p-type substrates. The corresponding values from the implanted and diffused samples presented in Section 3.1 are added for comparison, in the order of increasing doping concentration at the surface.

Blister densities (Fig. 5a) show a direct correlation with substrate resistivity. Densities are as low as only 0.5-1 blisters/ mm<sup>2</sup> for samples with high resistivity, and increase to 8/mm<sup>2</sup> and higher with decreasing resistivity, i.e. increasing bulk doping concentrations. Samples with phosphorus implantation and diffusion, however, show lower blister densities of  $\leq 3$  blisters/ mm<sup>2</sup> despite their significantly higher doping concentrations at the surface.

When examining the blister diameter (Fig. 5b) on the other hand, an opposite evolution is observed: substrates with higher resistivities suffer from very large blisters with average sizes of even  $>50$   $\mu\text{m}$ , while the average blister diameter is reduced to around 10  $\mu\text{m}$  as substrate resistivity decreases. Here, the behavior of implanted and diffused samples is more in line with this trend, with blister sizes of 20 and 4  $\mu\text{m}$ , respectively.

As a consequence of the negative correlation between blister diameter and density, the blistered surface area (Fig. 5c) does not change very clearly with resistivity. A decrease is observed over the studied substrate resistivity range, but the P-implanted sample and interestingly also the sample with 1-20  $\Omega\text{cm}$  resistivity, do not match this trend well. Despite the large diameters of blisters on high-resistivity substrates, the blisters are found to make up for only a small fraction of the total sample surface, below 0.35 % at maximum.

Blister properties and behavior in samples doped with boron are similar to those in samples doped with phosphorus, although this observation is based on fewer data points. Compared to the P-doped sample, the decrease in blister diameter for the sample with high boron doping appears to be slightly stronger, which is in line with the observations in Fig. 4.

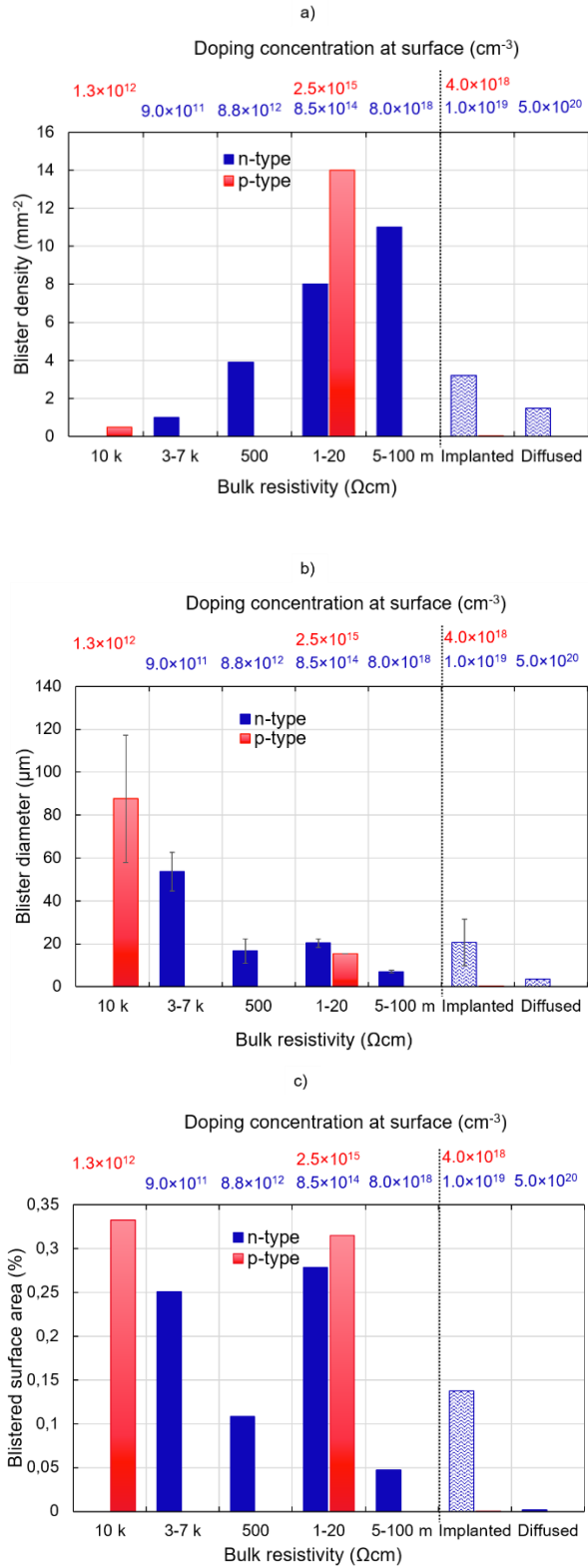


**Figure 5.** Blister densities (a), average blister diameters (b) and blistered surface area (c) for various substrate bulk resistivities. Electrically active dopant concentrations are represented as



median values for the corresponding resistivity range. Values for implanted and diffused samples from Section 3.1 are shown for reference on the right side of the dashed line.

As there are no previous reports on the blistering behavior of  $\text{Al}_2\text{O}_3$  with respect to either inactive or electrically active dopant concentration, comparison of the results obtained in this work with the literature is restricted to blister properties studied under the variation of other factors.

In general, the blister densities observed here are in line with earlier reports on  $\text{Al}_2\text{O}_3$  blistering, which present densities of less than 20 blisters per  $\text{mm}^2$ , at post-anneal temperatures below  $400\text{ }^\circ\text{C}$  that was also used in this work [14,15,20,31]. For blister diameters in  $\text{Al}_2\text{O}_3$ , the literature describes a wide range for varying conditions, from around  $5\text{ }\mu\text{m}$  to  $>100\text{ }\mu\text{m}$ . In all samples in this study, blister diameters fall into the same range, indicating that the absolute impact of total dopant concentration or electrically active doping of the substrate on blistering behavior is comparable to that of other, previously reported factors. A negative correlation between large blister size and high blister density, similar to the results obtained here for varying substrate resistivities, has been shown for blistered  $\text{Al}_2\text{O}_3$  stack systems deposited by spatial ALD and was attributed to a competition between lateral and vertical diffusion of hydrogen at the Si interface depending on post-anneal temperature, but no link to substrate doping was mentioned [32]. In absolute values, the blistered surface area has been reported with similar values, from 0.1 to 4 % depending on substrate treatment and post-anneal temperature [6,32], which are not in contradiction to the values between 0 and 0.35 % determined here. These values may seem rather low in general, but depending on the final desired properties and application of the  $\text{Al}_2\text{O}_3$  film, blisters may be harmful even when not covering larger surface areas.

From the above results, it is evident that also doping concentration as such, i.e. the bulk resistivity of the Si substrate, has an effect on the density and size of blisters in  $\text{Al}_2\text{O}_3$  films.

In Section 3.1, enhanced diffusion of hydrogen to point or cluster defects, reduction of the lateral diffusion of Si atoms on the surface due to dopant atoms and/or defects, and the increased surface hydrophilicity of highly doped surfaces in connection to the formation of a SiO<sub>2</sub> layer, were presented as potential mechanisms for the reduction of blistering due to external doping. As the condition of inactive phosphorus clusters or displacement damage is not given in crystals with doping already introduced during crystal growth, another mechanism must be responsible for the changes in blistering with varying resistivity. Hydrophilicity, in other words the termination of the substrate surface, has been observed to increase gradually over a wide range of surface doping concentrations [29,30], and is therefore deemed the most likely explanation for the observed blistering behavior. The commonly increased rates of chemical reactions, for example etching, in Si with higher total dopant concentration would be expected to have a stronger effect on the parameter of total blistered surface area, but may explain the shift towards higher blister density with simultaneously smaller blisters.

Considering especially the lower blister densities in the samples with high external doping concentration as well as the lower blister density, size, and total surface area observed for phosphorus diffusion compared to implantation, it is assumed that defects specific to the external doping methods do also provide an additional contribution to the reduction of blistering. To obtain conclusive evidence for or against either of these theories, more detailed information of the changes in defect states and chemical bonds at the Si surface and Si-Al<sub>2</sub>O<sub>3</sub> interface would be required. This would also shed more light on the role of the dopant species.

The relevance of different parameters used in blister characterization – density, size, total blistered surface area – is not unambiguous, and strongly depends on the device in which the Al<sub>2</sub>O<sub>3</sub> film is

applied. In a device with simple surface structure and efficiency influenced by the surface passivation, such as a solar cell, the total blistered area may be seen as the most critical parameter. On the other hand, in a segmented device with very fine pitch, *e.g.* a pixel detector, blister size must be monitored more closely: in order not to compromise the electrical insulation between electrodes (cf. Supporting Information, Section 2), blisters should be clearly smaller than the segment pitch. The final application also determines if a reduction of blistering by diffusion or implantation doping is feasible.

#### **4. Conclusions**

We have shown that the blistering of Al<sub>2</sub>O<sub>3</sub> thin films deposited by a TMA+H<sub>2</sub>O ALD process, which is well known to occur for example during the activation anneal of the passivation, is affected by doping in the silicon substrate. Both ion implantation and by diffusion were found to significantly reduce blistering in terms of blister size, density, and covered surface area, compared to the regions in the immediate vicinity without doping. Similar behavior is observed for both phosphorus and boron. Further investigation of this phenomenon using substrates with different resistivities revealed that even when introduced already during silicon crystal growth, doping affects the blistering of Al<sub>2</sub>O<sub>3</sub>. The reason for this is likely found in changes of the chemical properties of the silicon surface caused by high total dopant concentrations, promoting an –OH terminated surface and leading to the accelerated growth of an interfacial silicon oxide layer. In addition, cluster and point defects induced by diffusion or implantation, may contribute to the changes in blister properties and reduction in blistering.

The results obtained in this study show that doping concentration as such, i.e. the bulk resistivity of the Si substrate, has an effect on the density and size of blisters in Al<sub>2</sub>O<sub>3</sub> films, and a significant reduction of blistering can be achieved on substrates with very high doping concentrations, as are commonly obtained with ion implantation or diffusion. Substrate doping, whether referring to electrically active dopants or simply the presence of dopant atoms, thus represents one further factor, in addition to numerous substrate pre-treatments and Al<sub>2</sub>O<sub>3</sub> deposition process parameters reported in the literature, which affects blistering and can be used to reduce it.

## **Acknowledgements**

The authors acknowledge the provision of facilities and technical support for sample fabrication and characterization by Micronova Nanofabrication Centre and Nanomicroscopy Centre in Espoo, Finland within the OtaNano research infrastructure at Aalto University. The authors affiliated with Aalto University are part of the PREIN flagship of the Academy of Finland.

J. Ott would like to thank the Vilho, Yrjö and Kalle Väisälä Foundation of the Finnish Academy of Science and Letters for financial support. T. P. Pasanen acknowledges the Aalto ELEC Doctoral School, Jenny and Antti Wihuri Foundation, Walter Ahlström Foundation, and the Foundation of Electronic Engineers for the financial support. M. Garín acknowledges support from the project ENE2015-74009-JIN of the Spanish Ministry of Economy and Competitiveness (MINECO) and co-funded by the European Regional Development Fund.

Ms. Camilla Tossi is thanked for technical support with the microscope.

## ***Conflicts of Interest***

The authors declare no competing financial interest.

## ***References***

- [1] S.M. George, Atomic Layer Deposition: An Overview, *Chem. Rev.* **2010**, *110*, 111

- [2] G. Dingemans and W.M.M. Kessels, Status and prospects of Al<sub>2</sub>O<sub>3</sub>-based surface passivation schemes for silicon solar cells, *J. Vac. Sci. Technol. A* **2012**, *30*, 040802
- [3] M.A. Juntunen, J. Heinonen, V. Vähänissi, P. Repo, D. Valluru, H. Savin, Near-unity quantum efficiency of broadband black silicon photodiodes with an induced junction, *Nat. Photon.* **2016**, *10*, 777
- [4] J. Härkönen, E. Tuovinen, P. Luukka, A. Gädda, T. Mäenpää, E. Tuominen, T. Arsenovich, A. Junkes, X. Wu, Z. Li, Processing of n+/p-/p+ strip detectors with atomic layer deposition (ALD) grown Al<sub>2</sub>O<sub>3</sub> field insulator on magnetic Czochralski silicon (MCz-Si) substrates, *Nucl. Instrum. Methods Phys. Res. A* **2016**, *828*, 46
- [5] J. Ott, A. Gädda, S. Bharthuar, E. Brücken, M. Golovleva, J. Härkönen, M. Kalliokoski, A. Karadzhinova-Ferrer, S. Kirschenmann, V. Litichevskiy, P. Luukka, L. Martikainen, T. Naaranoja, Processing of AC-coupled n-in-p pixel detectors on MCz silicon using atomic layer deposited aluminium oxide, *Nucl. Instrum. Methods Phys. Res. A* **2019**, DOI: 10.1016/j.nima.2019.162547
- [6] B. Iandolo, R.S. Davidsen, O. Hansen, Avoiding blistering in Al<sub>2</sub>O<sub>3</sub> deposited on planar and black Si, *Sol. Energy Mater. Sol. Cells* **2018**, *187*, 23
- [7] M. Li, H.-S. Shin, K.-S. Jeong, S.-K. Oh, H. Lee, K. Han, G.-W. Lee, H.-D. Lee, Blistering Induced Degradation of Thermal Stability Al<sub>2</sub>O<sub>3</sub> Passivation Layer in Crystal Si Solar Cells, *Journal of Semiconductor Technology and Science* **2014**, *14*, 53
- [8] Z.-W. Peng, P.-T. Hsieh, Y.-J. Lin, C.-J. Huang, C.-C. Li, Investigation on blistering behavior for n-type silicon solar cells, *Energy Procedia* **2017**, *77*, 827
- [9] G. Kaur, N. Dwivedi, X. Zheng, B. Liao, L.Z. Peng, A. Danner, R. Stangl, C.S. Bhatia, Understanding Surface Treatment and ALD AlO<sub>x</sub> Thickness Induced Surface Passivation Quality of c-Si Cz Wafers, *IEEE Journal of Photovoltaics* **2017**, *7*, 1224
- [10] J. Ott, A. Gädda, M. Golovleva, T. Naaranoja, L. Martikainen, E. Brücken, V. Litichevskiy, A. Karadzhinova-Ferrer, M. Kalliokoski, P. Luukka, J. Härkönen, H. Savin, Detector processing on p-type MCz silicon using atomic layer deposition (ALD) grown aluminium oxide, 33rd RD50 workshop, 26-28 Nov 2018, CERN, Geneva, [https://indico.cern.ch/event/754063/contributions/3222806/attachments/1760772/2865963/JOtt\\_RD50\\_Nov18\\_3.pdf](https://indico.cern.ch/event/754063/contributions/3222806/attachments/1760772/2865963/JOtt_RD50_Nov18_3.pdf) (20.6.2019)
- [11] B. Vermang, H. Goverde, A. Uruena, A. Lorenz, E. Cornagliotti, A. Rothschild, J. John, J. Poortmans, R. Mertens, Blistering in ALD Al<sub>2</sub>O<sub>3</sub> passivation layers as rear contacting for local Al BSF Si solar cells, *Sol. Energy Mater. Sol. Cells* **2012**, *101*, 204
- [12] G. Dingemans, F. Einsele, W. Beyer, M.C.M. van de Sanden and W.M.M. Kessels, Influence of annealing and Al<sub>2</sub>O<sub>3</sub> properties on the hydrogen-induced passivation of the Si/SiO<sub>2</sub> interface, *J. Appl. Phys.* **2012**, *111*, 093713-1
- [13] G. Dingemans, W. Beyer, M. C. M. van de Sanden, W. M. M. Kessels, Hydrogen induced passivation of Si interfaces by Al<sub>2</sub>O<sub>3</sub> films and SiO<sub>2</sub>/Al<sub>2</sub>O<sub>3</sub> stacks, *Applied Phys. Lett.* **2010**, *97*, 152106
- [14] B. Vermang, H. Goverde, V. Simons, I. De Wolf, J. Meersschant, S. Tanaka, J. John, J. Poortmans and R. Mertens, A study of blister formation in ALD Al<sub>2</sub>O<sub>3</sub> grown on silicon, *38th IEEE Photovoltaic Specialists Conference* **2012**, 001135

- [15] M.C. Acero, O. Beldarrain, M. Duch, M. Zabala, M.B. González, F. Campabadal, Effect of the blistering of ALD Al<sub>2</sub>O<sub>3</sub> films on the silicon surface in Al-Al<sub>2</sub>O<sub>3</sub>-Si structures, *10th Spanish Conference on Electron Devices (CDE)* **2015**, 1
- [16] M. Broas, H. Jiang, A. Graff, T. Sajavaara, V. Vuorinen and M. Paulasto-Kröckel, Blistering mechanisms of atomic-layer-deposited AlN and Al<sub>2</sub>O<sub>3</sub> films, *Appl. Phys. Lett.* **2017**, *111*, 141606-1
- [17] T. Lüder, T. Lauer mann, A. Zuschlag, G. Hahn, B. Terheiden, Al<sub>2</sub>O<sub>3</sub>/SiN<sub>x</sub> stacks at increased temperatures: avoiding blistering during contact firing, *Energy Procedia* **2012**, *27*, 426
- [18] S. Li, P. Repo, G. von Gastrow, Y. Bao, H. Savin, Effect of ALD Reactants on Blistering of Aluminum Oxide Films on Crystalline Silicon, *IEEE 39th Photovoltaic Specialists Conference (PVSC)* **2013**, 1265
- [19] X. Gay, F. Souren, B. Dielissen, M. Bijker, R. Gortzen, D. Pysch, K. Weise, B. Sander, R. Sastrawan, Post-deposition thermal treatment of ultrafast spatial ALD Al<sub>2</sub>O<sub>3</sub> for the rear side passivation of p-type solar cells, *28th EUPVSEC* **2013**
- [20] O. Beldarrain, M. Duch, M. Zabala, J.M. Rafí, M. Bargalló González and F. Campabadal, Blistering of atomic layer deposition Al<sub>2</sub>O<sub>3</sub> layers grown on silicon and its effect on metal-insulator-semiconductor structures, *J. Vac. Sci. Technol. A* **2013**, *31*, 01A128-1
- [21] Y. Bao, S. Li, G. von Gastrow, R. Repo, H. Savin, M. Putkonen, Effect of substrate pretreatments on the atomic layer deposited Al<sub>2</sub>O<sub>3</sub> passivation quality, *J. Vac. Sci. Technol. A* **2015**, *33*, 01A123-1
- [22] W. Kern, D. A. Puotinen, RCA Cleaning, *RCA Reviews* **1970**, *31*, 187
- [23] T.P. Pasanen, V. Vähänissi, N. Theut, H. Savin, Surface passivation of black silicon phosphorus emitters with atomic layer deposited SiO<sub>2</sub>/Al<sub>2</sub>O<sub>3</sub> stacks, *Energy Procedia* **2017**, *124*, 307
- [24] L.V.C. Assali, J.R. Leite, Microscopic Mechanism of Hydrogen Passivation of Acceptor Shallow Levels in Silicon, *Phys. Rev. Lett.* **1985**, *55*, 980
- [25] N.M. Johnson, C. Herring, D.J. Chadi, Interstitial Hydrogen and Neutralization of Shallow-Donor Impurities in Single-Crystal Silicon, *Phys. Rev. Lett.* **1986**, *56*, 769
- [26] N.M. Johnson, S.K. Hahn, Hydrogen passivation of the oxygen-related thermal-donor defect in silicon, *Appl. Phys. Lett* **1986**, *48*, 709
- [27] N. Fukata, S. Sasaki, S. Fujimura, H. Haneda, K. Murakami, Hydrogen Passivation of Donors and Hydrogen States in Heavily Doped n-type Silicon, *Jpn. J. Appl. Phys.* **1996**, *35*, 3937
- [28] M.D. McCluskey, E.E. Haller, *Dopants and Defects in Semiconductors*, CRC Press, Boca Raton, FL, USA **2012**
- [29] Y. Sato and M. Maeda, Study of HF-Treated Heavily-Doped Si Surface Using Contact Angle Measurements, *Jpn. J. Appl. Phys.* **1994**, *33*, 6508
- [30] M. Morita, T. Ohmi, E. Hasegawa, M. Kawakami, M. Ohwada, Growth of native oxide on a silicon surface, *J. Appl. Phys.* **1990**, *68*, 1272
- [31] B. Vermang, H. Goverde, A. Lorenz, A. Uruena, G. Vereecke, J. Meersschaut, E. Cornagliotti, A. Rothschild, J. John, J. Poortmans, R. Mertens, On the blistering of atomic layer deposited Al<sub>2</sub>O<sub>3</sub> as Si surface passivation, *37th IEEE Photovoltaic Specialists Conference* **2011**, 003562

[32] L. Hennen, E.H.A. Granneman, W.M.M. Kessels, Analysis of Blister Formation in Spatial ALD Al<sub>2</sub>O<sub>3</sub> for Silicon Surface Passivation, *38th IEEE Photovoltaic Specialists Conference* **2012**, 001049